

Timing of pulsars found in a deep Parkes multibeam survey

D. R. Lorimer^{1,2,3,*}, F. Camilo^{4,5} and M. A. McLaughlin^{1,3}

¹ *Department of Physics, West Virginia University, PO Box 6315, Morgantown, WV 26506, USA*

² *National Radio Astronomy Observatory, PO Box 2, Green Bank, WV 24944, USA*

³ *Astrophysics, University of Oxford, Denys Wilkinson Building, Keble Road, Oxford OX1 3RH*

⁴ *Columbia Astrophysics Laboratory, Columbia University, 550 West 120th Street, New York, NY 10027, USA*

⁵ *National Aeronomy and Ionospheric Center, Arecibo Observatory, HC 3 Box 53995, Arecibo, PR 00612, USA*

Accepted for publication in MNRAS

ABSTRACT

We have carried out a sensitive radio pulsar survey along the northern Galactic plane ($50^\circ < l < 60^\circ$ and $|b| \lesssim 2^\circ$) using the Parkes 20-cm multibeam system. We observed each position for 70-min on two separate epochs. Our analyses to date have so far resulted in the detection of 32 pulsars, of which 17 were previously unknown. Here we summarize the observations and analysis and present the timing observations of 11 pulsars and discovery parameters for a further 6 pulsars. We also present a timing solution for the 166-ms bursting pulsar, PSR J1938+2213, previously discovered during an Arecibo drift-scan survey. Our survey data for this pulsar show that the emission can be described by a steady pulse component with bursting emission, which lasts for typically 20–25 pulse periods, superposed. Other new discoveries are the young 80.1-ms pulsar PSR J1935+2025 which exhibits a significant amount of unmodeled low-frequency noise in its timing residuals, and the 4.2-ms pulsar PSR J1935+1726 which is in a low-mass binary system with a 90.7-day circular orbit.

Key words: pulsars: general — pulsars: searches — pulsars: timing — stars: neutron

1 INTRODUCTION

With over 800 new pulsar discoveries, primarily in the region defined by Galactic coordinates $-100^\circ < l < 50^\circ$ and $|b| < 5^\circ$, the Parkes Multibeam Pulsar Survey (Manchester et al. 2001) is the most successful large-scale search for pulsars to date. The survey, with 35-minute pointings, has been a fantastic probe of the Galactic pulsar population and has resulted in the discovery of numerous interesting individual systems (see, e.g., Lyne 2009 for a review). Motivated by the high density of young pulsars in the range $|b| < 1^\circ$ (see, e.g., Camilo 2004), in 2004–2005 we extended the coverage by surveying the most northerly Galactic longitudes possible from Parkes using 70-minute pointings in the range $50^\circ < l < 60^\circ$ and $|b| \lesssim 2^\circ$. This region is also being covered by the Pulsar Arecibo L-band Feed Array survey (Cordes et al. 2006), and the Effelsberg High Time Resolution Universe survey (Barr et al., submitted). Our analyses to date have resulted in the discovery of 17 new pulsars and a further 15 that were previously known. In §2 we summarize the survey observations and analyses so far, and present the timing parameters and pulse profiles from observations of the newly discovered pulsars. We discuss these results in §3 and present our conclusions in §4.

2 DISCOVERY AND TIMING OBSERVATIONS

We summarize the survey observations and data analysis procedures which led to the discovery of the pulsars presented in this paper. The survey observations were conducted between 2004 September 22 and 2005 April 20 using the 20-cm multibeam receiver at the Parkes 64-m telescope. A total of 120 multibeam pointings were observed in the survey region approximately defined by Galactic longitudes in the range $50^\circ \lesssim l \lesssim 60^\circ$ and Galactic latitudes in the range $|b| \lesssim 2^\circ$. Each sky position was observed for 70 minutes at two different epochs, i.e. the entire survey region was covered twice. Radio-frequency signals from each beam were acquired using the analog filterbank system described by Manchester et al. (2001). The incoming data were sampled every 125 μs with 1-bit precision over 96 adjacent frequency channels each of width 3 MHz. The survey integration time and sampling rate on each pass was twice that of the original multibeam survey (Manchester et al. 2001).

An initial analysis of the data was performed shortly after collection at Parkes on local computers using a pipeline based on the SIGPROC processing software¹. To speed up the overall processing time, the data were downsampled by adding eight adjacent time samples together to form 96

* Email: Duncan.Lorimer@mail.wvu.edu

¹ <http://sigproc.sourceforge.net>

Table 1. Astrometric and spin parameters for the 18 pulsars described in this paper. For the 12 pulsars for which timing observations have been carried out, we also give the MJD of the epoch used for period determination, the number of individual TOAs (N) included in the timing solution, the MJD range covered and the root-mean-square (RMS) of the post-fit timing residuals. Figures in parentheses represent $1\text{-}\sigma$ uncertainties in the least significant digit(s) as reported by TEMPO.

PSR J	R.A. (J2000)	Dec. (J2000)	Period, P (ms)	\dot{P} (10^{-15})	Epoch (MJD)	N	Data span (MJD)	RMS (ms)
1919+1645	19:19:09.243(2)	16:45:22.72(8)	562.789986697(3)	0.2161(4)	53560	68	53286–53834	2.1
1921+1544	19:21:46.4723(9)	15:44:17.46(2)	143.5756814094(2)	0.98036(2)	53632	49	53347–53916	0.6
1922+1733	19:22:53.2180(7)	17:33:23.47(2)	236.1708772317(3)	13.38394(4)	53595	108	53273–53916	1.2
1924+1639	19:24:03.1115(5)	16:39:40.756(9)	158.0429177826(2)	2.56384(1)	53720	123	53272–53916	1.1
1925+19	19:25:26(28)	19:04(7)	1916.353(6)		54346			
1926+2016	19:26:18.064(1)	20:16:01.13(3)	299.0717782966(7)	3.50084(6)	53595	72	53271–53916	1.6
1928+1923	19:28:05.163(5)	19:23:31.32(8)	817.329808312(6)	6.3495(7)	53640	125	53360–53916	2.2
1929+16	19:29:18(28)	16:21(7)	529.681(2)		53480			
1929+19	19:29:32(28)	19:05(7)	339.2154(4)		53363			
1929+1955	19:29:17.5713(6)	19:55:07.91(1)	257.8319398983(3)	2.55530(3)	53595	308	53271–53916	1.0
1929+2121	19:29:04.239(2)	21:21:22.68(3)	723.598503258(2)	2.1386(2)	53635	91	53355–53916	0.3
1930+17	19:30:44(28)	17:25(7)	1609.6903(7)		53443			
1931+1952	19:31:55.864(3)	19:52:11.5(1)	501.123112694(4)	0.1008(6)	53560	29	53285–53834	0.8
1935+1726	19:35:03.948(3)	17:26:28.46(3)	4.200101791882(7)	< 0.00001	55314	23	55112–55514	0.049
1935+2025	19:35:41.941(3)	20:25:40.1(3)	80.118133455(6)	60.7579(1)	53460	109	53271–53650	0.3
1936+21	19:36:29(28)	21:12(7)	642.932(2)		53281			
1938+20	19:38:12(28)	20:10(7)	687.0804(1)		53286			
1938+2213	19:38:14.180(3)	22:13:12.68(4)	166.1155731566(6)	42.4423(5)	53500	79	53346–53651	0.8

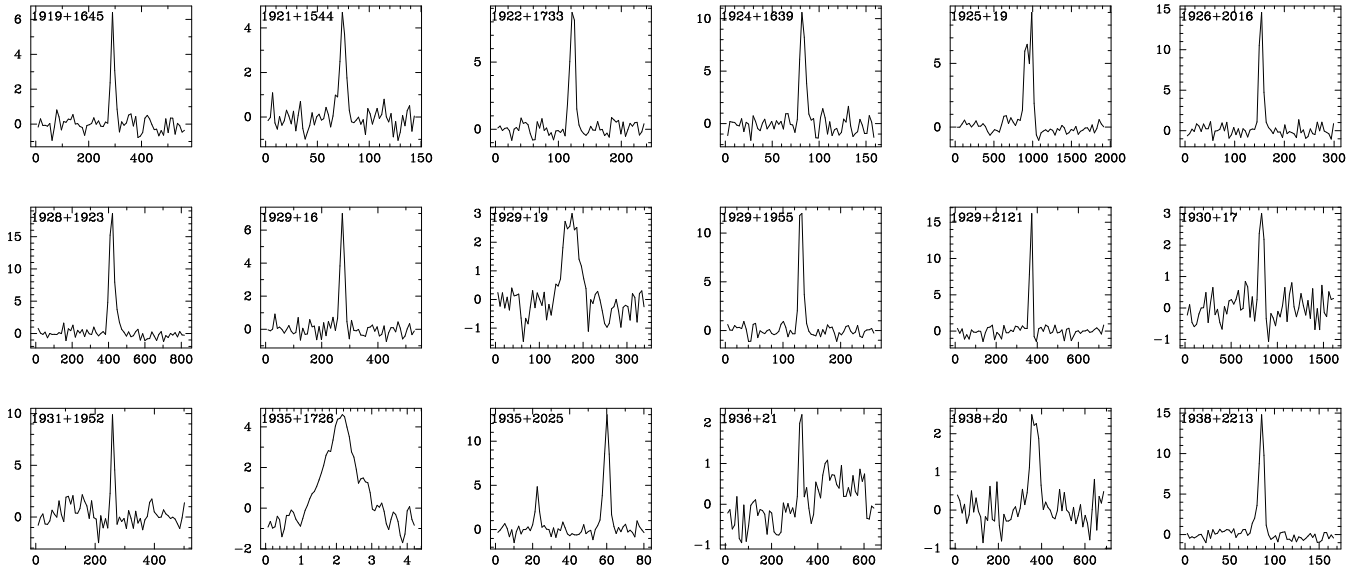


Figure 1. Integrated pulse profiles for all 17 pulsars discovered in the survey, as well as PSR J1938+2213. The horizontal axis shows pulse phase in ms and the vertical axis is flux density in mJy. These data were obtained by folding one of the survey observations for each pulsar.

channel filterbank files with 1 ms time resolution. The effects of the interstellar medium were compensated for by de-dispersing data from each telescope beam at 496 different trial values of dispersion measure (DM) spanning the range 1.1 and 4931 cm^{-3} pc. The de-dispersed time series were then subjected to a standard Fourier analysis to search for periodic signals (Lorimer & Kramer 2005) and a search for dispersed single pulses (McLaughlin et al. 2006). Pulsar candidates were selected by eye from inspection of diagnostic plots showing the properties of each candidate. The two passes of the survey region allowed us to confirm the existence of each pulsar reported in this paper by inspecting the corresponding output of the second observation. This initial processing resulted in the discovery of 12 pulsars. A second pass of the data using the same pipeline, but with full time resolution, resulted in the discovery of a further five pulsars including the millisecond pulsar J1935+1726. For all pulsars found so far, the data have been folded in turn at two and three times the tabulated periods to confirm that they represent the fundamental periods of the pulsars, rather than a harmonic.

Timing solutions have so far been obtained for 11 of the newly discovered pulsars as well as PSR J1938+2213 which was previously discovered (but not further studied to our knowledge) during a drift-scan survey with the Arecibo telescope (Chandler 2003). These have been obtained from the analysis of a series of observations carried out with the Parkes telescope and Green Bank Telescope. At Parkes, we used the analogue filterbanks to acquire the data in an identical fashion to that described by Manchester et al. (2001) and Morris et al. (2002) respectively. The Green Bank timing made use of the SPIGOT and (for J1935+1726) GUPPI data acquisition systems described by Kaplan et al. (2005) and DuPlain et al. (2008) respectively. For each pulsar, pulse times of arrival (TOAs) were determined from the individual observations using standard techniques (see, e.g., Lorimer & Kramer 2005) implemented in the PRESTO software package². A model containing the spin, astrometric and (if necessary) any binary parameters was fitted to the TOAs using the TEMPO timing package³. The basic astrometric and spin information from this analysis is provided in Table 1. For the six pulsars which have so far not been timed, only their discovery information (i.e. approximate position, barycentric period and dispersion measure) are provided. Dispersion measures and their quoted uncertainties are derived from the discovery observations. Specifically, the uncertainties are calculated by requiring that the pulse must drift by less than one phase bin due to any incorrect dispersion across the 288 MHz band.

Our follow-up observations of PSR J1935+1726 showed changes in the barycentric spin period from epoch to epoch that were consistent with the Doppler modulation due to binary motion of the pulsar. A fit to the barycentric periods revealed a 90.7 day period for a circular orbit with a semi-major axis of 31.97 light seconds. Once this orbit was included in the timing analysis, we were able to obtain a fully coherent fit using TEMPO. As is now common practice for low-eccentricity binary systems, we used the “ELL1” bi-

Table 2. Orbital parameters for PSR J1935+1726 obtained using the “ELL1” binary model (Lange et al. 2001). Figures in parentheses represent 1- σ uncertainties in the least significant digit(s) and are the nominal uncertainties reported by TEMPO. We also list the equivalent orbital eccentricity, as derived from the Laplace-Lagrange parameters (see Lange et al. 2001 for details).

Orbital period (d)	90.76389(2)
Projected semi-major axis of orbit (lt sec)	31.97423(6)
First Laplace-Lagrange parameter	0.000031(4)
Second Laplace-Lagrange parameter	0.000173(4)
Epoch of ascending node (MJD)	54616.7206(1)
Orbital eccentricity	0.000176(4)

nary model using the Laplace–Lagrange parameterization of the eccentricity (Lange et al. 2001) in this fit. The resulting parameters are given in Table 2 and discussed below in § 3.2.

In addition to the timing analyses, we also carried out preliminary measurements of pulse width and flux densities for each pulsar using the survey data. The results of these measurements are given in Table 2. Pulse widths were measured at 50% and 10% of the main pulse (W_{50} and W_{10} respectively) as well as the equivalent width (W_{eq}) which is defined to be the width of a top-hat pulse with the same area and peak flux density as the observed profile. The millijansky scale for the flux density calculations was established from the off-pulse RMS using the radiometer equation (e.g., Lorimer & Kramer 2005) and adopting the Parkes multibeam system parameters from Manchester et al. (2001). For each profile, we quote the peak flux density (S_{peak}) and calculated the mean flux density (S_{mean}) by integrating each profile and dividing by the number of bins. To account for the position offset r between the search-mode observation and the timing position, we assumed a Gaussian beam with half-power beamwidth w and multiplied the flux densities by the factor $\exp(2.77r^2/w^2)$ as described by Lorimer et al. (2006). For those pulsars whose positions are not accurately determined from timing measurements, this correction is not made, and the tabulated flux densities and corresponding luminosities are lower limits.

3 DISCUSSION

3.1 Derived parameters

Various derived parameters for the new pulsars are presented in Table 3. For each pulsar, when known, we list the base-10 logarithms of the characteristic age, surface dipole magnetic field strength and rate of loss of rotational energy. The final columns contain the pulsar distances and height above the Galactic plane computed from their DMs assuming the Cordes & Lazio (2002) models for the Galactic distribution of free electrons. As a group, these pulsars have consistent properties to the larger samples published in the main multibeam survey. We note that some of the distances (e.g. 15.3 kpc for PSR J1929+19) may be significantly overestimated due to uncertainties in the electron density model for this part of the Galactic plane.

Also listed in Table 3 are the flux densities and the corresponding pseudoluminosity estimates (i.e. flux times distance squared), or lower limits thereof, as appropriate.

² <http://www.cv.nrao.edu/~sransom/presto>

³ <http://tempo.sourceforge.net>

Table 3. Observed and derived parameters for the 18 pulsars presented in this paper. Listed the Galactic longitude, l , Galactic latitude, b (both in degrees), DM (cm^{-3} pc), pulse width at 50% and 10% of the peak and the equivalent width (respectively W_{50} , W_{10} and W_{eq} all in ms), peak and mean 1400-MHz flux density (mJy), the base-10 logarithms of characteristic age (yr), the surface dipole magnetic field strength (G), the loss in rotational energy (erg s^{-1}), the DM-derived distance using the Cordes & Lazio (2001) model, D (kpc), the height with respect to the Galactic plane, z (pc) and the 1400-MHz pseudoluminosity (mJy kpc^2).

PSR J	l	b	DM	W_{50}	W_{10}	W_{eq}	S_{peak}	S_{mean}	$\log[\tau_c]$	$\log[B]$	$\log[\dot{E}]$	D	z	L_{1400}
1919+1645	51.0	1.6	208(9)	14.5	35.0	13.7	6.4	0.16	7.6	11.5	31.7	6.8	200	7.4
1921+1544	50.4	0.6	385(2)	6.3	13.7	0.4	4.7	0.01	6.4	11.6	34.1	13.1	140	1.7
1922+1733	52.1	1.2	238(4)	9.4	16.7	8.3	8.7	0.31	5.4	12.3	34.6	7.4	160	17
1924+1639	51.4	0.6	208(3)	7.2	10.9	7.6	10.6	0.51	6.0	11.8	34.4	6.6	65	22
1925+19	53.7	1.4	328(16)	—	130.2	55.5	> 9	> 0.5				9.8	250	> 48
1926+2016	54.9	1.8	247(5)	9.7	18.0	13.1	14.6	0.64	6.1	12.0	33.7	8.1	260	42
1928+1923	54.3	1.0	476(14)	30.9	71.2	30.7	18.6	0.70	6.3	12.4	32.7	14.1	480	140
1929+16	51.7	-0.7	12(9)	20.6	32.9	24.4	> 7	> 0.3				1.3	-14	> 0.5
1929+19	54.2	0.6	527(6)	38.4	69.6	8.1	> 3	> 0.06				15.3	180	> 14
1929+1955	54.9	1.0	281(4)	10.2	16.4	7.1	12.0	0.33	6.2	11.9	33.7	8.8	160	26
1929+2121	56.1	1.8	66(12)	15.0	33.0	10.3	16.2	0.23	6.7	12.1	32.3	3.4	100	2.7
1930+17	52.8	-0.5	201(27)	68.6	93.4	111.0	> 3	> 0.2				6.4	-37	> 8
1931+1952	55.1	0.5	441(8)	13.0	22.4	16.9	9.9	0.33	7.9	11.4	31.5	12.6	100	52
1935+1726	53.4	-1.4	61.6(1)	0.8	1.7	0.6	4.6	0.68				3.2	-76	7
1935+2025	56.1	-0.1	182(1)	3.7,2.4	6.7,4.5	4.9	13.0	0.79	4.3	12.3	36.7	6.2	-6	30
1936+21	56.8	0.2	264(11)	19.2	31.2	30.3	> 2.2	> 0.03				8.4	38	> 2
1938+20	56.1	-0.7	306(12)	47.9	79.1	50.4	> 2.5	> 0.2				9.3	-110	> 17
1938+2213	57.9	0.3	91(3)	6.8	15.1	6.6	14.8	0.59	4.8	12.4	35.5	4.1	22	10

While these are generally weak sources, with 1400-MHz flux densities as low as $10 \mu\text{Jy}$, because of their large distances, the pulsars' radio luminosities are not unusually low when compared with the rest of the known population.

3.2 PSR J1935+1726

This 4.2 ms pulsar is one of two millisecond pulsars detected from an analysis of the survey observations so far. The other detection was the original millisecond pulsar, B1937+21 (Backer et al. 1982). While the timing precision we have been able to achieve from PSR J1935+1726 ($\sim 50 \mu\text{s}$ RMS) will mean that it is unlikely to warrant consideration into pulsar timing arrays (e.g., Demorest et al. 2013), it does permit a precise determination of the orbital parameters. From these data provided in Table 2, the Keplerian mass function for this system is $4.26 \times 10^{-3} M_{\odot}$. This is a typical value for millisecond pulsar binaries in which the companion star is expected on evolutionary grounds to be a low-mass white dwarf (see, e.g., Lorimer 2008). Assuming a millisecond pulsar mass of $1.5 M_{\odot}$ (Özel et al. 2012), and an orbital inclination angle of 90° , we infer the companion star's mass to be $> 0.23 M_{\odot}$. The orbital eccentricity for this system (1.76×10^{-4}) listed in Table 2 is entirely consistent with the value predicted from the orbital period by the fluctuation-dissipation theory developed by Phinney (1992). This has been noted for many other (but not all, Burgay et al. 2013) millisecond pulsar binaries, suggesting that PSR J1935+1736 has followed a standard low-mass binary evolution to evolve to its presently observed state.

3.3 PSR J1935+2025

This 80.1 ms pulsar has the lowest characteristic age of all the new discoveries ($\tau_c \approx 21,000$ yr), and is the only pulsar in which an interpulse is clearly detectable (Fig. 1). No known supernova remnant, X-ray or gamma-ray source exists at the pulsar's position. There is a significant amount of unmodeled behaviour still present in the timing residuals. This can be largely removed by fitting for a second frequency derivative of $\dot{\nu} = (2.93 \pm 0.06) \times 10^{-22} \text{ s}^{-3}$. When interpreted in terms of the standard power-law spindown model where $\dot{\nu} \propto \nu^n$, for a braking index n and spin frequency ν (e.g., Lorimer & Kramer 2005), the implied braking index $n = \nu\dot{\nu}/(\dot{\nu})^2 = 40.8$ is well outside the range expected for long-term spin behaviour (e.g., Johnston & Galloway 1999) and most likely suggests the presence of significant low-frequency noise in this pulsar.

3.4 PSR J1938+2213

This 166-ms pulsar was discovered by Chandler (2003) in a 430-MHz drift scan survey with the Arecibo telescope. As noted by Chandler, this source is unusual in that it exhibits short timescale bursting behaviour. This emission is seen clearly in one of the survey pointings shown in Fig. 2. Each pulse phase bin shown in this image has been smoothed using a boxcar of width 64 pulses running vertically to enhance the average emission seen around pulse phase bin number 15. A total of 12 bursting events, lasting typically 20–25 pulse periods, can be seen in this image. As the integrated profiles in the inset to this figure show, the bursting events

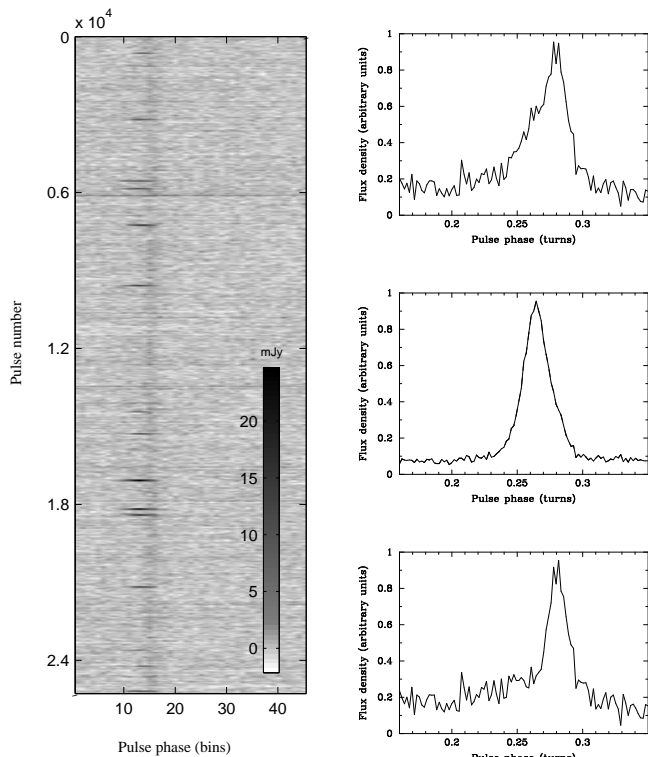


Figure 2. Left: observing time versus pulse phase in bins for one of the survey pointings for PSR J1938+2213 showing bursting events during the 70-min observation. Right: integrated pulse profiles showing 20% of the period around the main pulse for (top) the entire observation, (middle) the bright bursts minus the average faint emission, (bottom) the faint emission only. The millijansky scale was established using the radiometer noise as described in Section 2.

are clearly offset from the main profile in pulse phase. Thus the emission process in this pulsar appears to consist of a steady emission mode superposed by these brighter bursts. Our understanding of these bursting pulsars is currently limited by studies of only a few sources (Nowakowski 1992; Lewandowski et al. 2004; Seymour et al. 2013). Further examples of this phenomenon, as well as more sensitive observations, are clearly required to improve our understanding of the complex emission physics of neutron stars.

4 CONCLUSIONS

We have carried out a deep survey of the northern Galactic plane using the Parkes radio telescope and have discovered 17 new pulsars. Among the new discoveries is the binary millisecond pulsar PSR J1935+1726 and the young 80.1-ms pulsar PSR J1935+2025. Our follow up timing observations have provided phase-connected timing solutions for 11 of these pulsars, as well as a solution for the previously known bursting pulsar PSR J1938+2213. Our survey observation of this pulsar reveal that the bursting emission is superposed over a fainter, steadier, emission region which is offset in pulse phase from the bursts.

A novel feature of our survey was that we carried out two observations of each sky position. All of the discoveries made here were visible in both survey observations. Further

processing of the data in future will search for fainter candidates which might appear in both survey pointings, but at a lower significance than would otherwise be believable from an analysis of a single survey pointing. So far, our processing has not accounted for the effects of any orbital motion which may be significant during the 70-min pointings. An acceleration search analysis will shortly be carried out and the results of this search will be published elsewhere.

ACKNOWLEDGMENTS

The Parkes radio telescope is part of the Australia Telescope which is funded by the Commonwealth of Australia for operation as a National Facility managed by CSIRO. The National Radio Astronomy Observatory is a facility of the National Science Foundation operated under cooperative agreement by Associated Universities, Inc. This work made use of the facilities of the ATNF Pulsar Catalogue, the SAO/NASA Astrophysics Data System and the HEASARC archival data search tool. DRL acknowledges support from the Royal Society as a University Research Fellow during the early phases of this project. We thank Matthew Bailes for making his computing facilities at Parkes available for the initial search processing. Computer resources used during the later stages of this project were supported from a WV EPSCoR Challenge Grant awarded to DRL and MAM. We thank Andrew Seymour for producing Figure 2, and West Virginia University undergraduates Austin Anuta-Darling and Adil Moghal for data processing assistance during the course of this work. DRL and MAM acknowledge support from Oxford Astrophysics while on sabbatical leave.

REFERENCES

- Backer D. C., Kulkarni S. R., Heiles C., Davis M. M., Goss W. M., 1982, *Nature*, 300, 615
 Burgay M. et al., 2013, *MNRAS*, 429, 579
 Camilo F., 2004, in *IAU Symposium*, Vol. 218, *Young Neutron Stars and Their Environments*, Camilo F., Gaensler B. M., eds., p. 97
 Chandler A. M., 2003, PhD thesis, California Institute of Technology
 Cordes J. M. et al., 2006, *ApJ*, 637, 446
 Cordes J. M., Lazio T. J. W., 2002, *astro-ph/0207156*
 Demorest P. B. et al., 2013, *ApJ*, 762, 94
 DuPlain R., Ransom S., Demorest P., Brandt P., Ford J., Shelton A. L., 2008, in *Society of Photo-Optical Instrumentation Engineers (SPIE) Conference Series*, Vol. 7019, *Society of Photo-Optical Instrumentation Engineers (SPIE) Conference Series*
 Johnston S., Galloway D., 1999, *MNRAS*, 306, L50
 Kaplan D. L. et al., 2005, *PASP*, 117, 643
 Lange C., Camilo F., Wex N., Kramer M., Backer D., Lyne A., Doroshenko O., 2001, *MNRAS*, 326, 274
 Lewandowski W., Wolszczan A., Feiler G., Konacki M., Sołtysiński T., 2004, *ApJ*, 600, 905
 Lorimer D. R., 2008, *Living Reviews in Relativity*, 11
 Lorimer D. R. et al., 2006, *MNRAS*, 372, 777
 Lorimer D. R., Kramer M., 2005, *Handbook of Pulsar Astronomy*. Cambridge University Press

- Manchester R. N. et al., 2001, MNRAS, 328, 17
McLaughlin M. A. et al., 2006, Nature, 439, 817
Morris D. J. et al., 2002, MNRAS, 335, 275
Nowakowski L. A., 1992, in IAU Colloq. 128: Magnetospheric Structure and Emission Mechanics of Radio Pulsars, Hankins T. H., Rankin J. M., Gil J. A., eds., p. 280
Özel F., Psaltis D., Narayan R., Santos Villarreal A., 2012, ApJ, 757, 55
Phinney E. S., 1992, Philos. Trans. Roy. Soc. London A, 341, 39
Seymour A., Lorimer D. R., Ridley J. P., 2013, MNRAS, submitted